Antiferroelectric-like properties and enhanced polarization of Cu-doped K0.5Na0.5NbO3 piezoelectric ceramics

S. M. Ke, H. T. Huang, H. Q. Fan, H. K. Lee, L. M. Zhou et al.

Related Articles

The impact of the Pb(Zr,Ti)O3-ZnO interface quality on the hysteretic properties of a metal-ferroelectric-semiconductor structure
J. Appl. Phys. 112, 104103 (2012)

Ferroelectric properties of Pb(Zr,Ti)O3 films under ion-beam induced strain
J. Appl. Phys. 112, 104111 (2012)

Ferroic states and phase coexistence in BiFeO3-BaTiO3 solid solutions
J. Appl. Phys. 112, 104112 (2012)

Single-crystalline BiFeO3 nanowires and their ferroelectric behavior
Appl. Phys. Lett. 101, 192903 (2012)

Role of measurement voltage on hysteresis loop shape in Piezoresponse Force Microscopy
Appl. Phys. Lett. 101, 192902 (2012)

Additional information on Appl. Phys. Lett.

Journal Homepage: http://apl.aip.org/

Journal Information: http://apl.aip.org/about/about_the_journal

Top downloads: http://apl.aip.org/features/most_downloaded

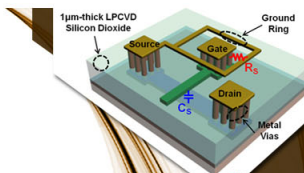Information for Authors: http://apl.aip.org/authors

Antiferroelectric-like properties and enhanced polarization of Cu-doped $K_{0.5}Na_{0.5}NbO_3$ piezoelectric ceramics

S. M. Ke,[1,2] H. T. Huang,[3,a)] H. Q. Fan,[4] H. K. Lee,[5] L. M. Zhou,[2] and Y.-W. Mai[2,6]

[1]*College of Materials Science and Engineering, Shenzhen University, Shenzhen 518060, China*
[2]*Department of Mechanical Engineering, The Hong Kong Polytechnic University, Hong Kong*
[3]*Department of Applied Physics, The Hong Kong Polytechnic University, Hong Kong*
[4]*School of Materials Science and Engineering, Northwestern Polytechnical University, Xi'an 710072, China*
[5]*Department of Chemistry, The Chinese University of Hong Kong, Hong Kong*
[6]*Center for Advanced Materials Technology (CAMT), School of Aerospace, Mechanical and Mechatronic Engineering J07, University of Sydney, Sydney NSW 2006, Australia*

Abnormal evolution of ferroelectric hysteresis (*P-E*) loops was observed in Cu-doped $K_{0.5}Na_{0.5}NbO_3$ (KNN) ceramics. The 1 mol.% Cu-doped fresh sample exhibited double-loop-like characteristics, while the 1.5 and 2 mol.% Cu-doped KNN ceramics showed normal single loops. Electron paramagnetic resonance spectra verified the formation of non-switchable $(Cu'''_{Nb} - V^{\bullet\bullet}_O)'$ (DC1) and non-polar $(V^{\bullet\bullet}_O - Cu'''_{Nb} - V^{\bullet\bullet}_O)^{\bullet}$ (DC2) defect complexes in these ceramics. According to the experimental results, it is suggested that DC1 would provide the driving force for domain back-switching, leading to the double *P-E* loops, while DC2 would contribute to the space charges. Dielectric aging behaviors of the samples also supported this mechanism. It is the competition between the DC1 and DC2 defect complexes that induced the observed compositional evolution of *P-E* loops in the Cu-doped KNN ceramics. © *2012 American Institute of Physics*.
[http://dx.doi.org/10.1063/1.4747212]

As a typical feature, double polarization-electric field (*P-E*) hysteresis loops have been observed in many acceptor-doped ferroelectrics (FEs), such as Mn-doped $BaTiO_3$ after aging.[1,2] The aging effects in FEs include spontaneous time-dependent variations in *P-E* loop, electro-strain, dielectric and piezoelectric characteristics, etc. Two competing mechanisms involving charge carriers and their interaction with polarization have been proposed to explain the FE aging. One is based on the formation and reorientation of defect dipoles, i.e., charge carrier migration in the unit cell (volume effect).[2,3] The other is based on the migration of charges to domain walls,[4,5] grain boundaries,[6] or sample surface[7] (interface effect) to stabilize a certain domain configuration. The double *P-E* loops are then caused by the resulting constriction of the polarization. Recent studies revealed that more than one process of aging may be active in one material.[8,9]

Since the volume effect is related to the migration of charged carriers, both the thermodynamic and kinetic behaviors of these carriers should be considered. The crucial role played by the migration kinetics of point defects has been demonstrated in Al^{3+}-doped $BaTiO_3$ ceramics,[10] where the Al^{3+}-doping leads to lattice shrinkage and suppresses the FE aging effect at high level doping. Moreover, double *P-E* loops have also been reported in some acceptor-doped ferroelectrics *without* aging, such as in K^+-doped $PbZr_xTi_{1-x}O_3$ (PZT)[11,12] and Cu^{2+}-doped $K_{0.5}Na_{0.5}NbO_3$ (KNN) ceramics.[13] This phenomenon has been explained on the basis of the high mobility of defect dipoles, which could reorient easily after the formation of domain patterns.[11–13] Accordingly, aging is not required for the ceramics to exhibit

double *P-E* loops. In the present work, we studied the *P-E* loops and dielectric aging behaviors of KNN ceramics with Cu doping. Interestingly, it is found that, contrary to the double *P-E* loop characteristics of the 1 mol.% Cu doped sample, the KNN ceramics with higher doping levels showed normal hysteresis loops with significantly enhanced polarization.

Ceramics with nominal composition $K_{0.5}Na_{0.5}$ $(Nb_{1-2x/5}Cu_x)O_3$ ($x = 0$, 0.0025, 0.005, 0.0075, 0.01, 0.0125, 0.015, 0.0175, and 0.02, respectively, abbreviated as KNN1000x) were prepared by using the conventional solid state reaction method. Analytical reagents of K_2CO_3, Na_2CO_3, Nb_2O_5, and CuO were mixed by using a planetary ball mill with anhydrous ethanol as the medium and then calcined at 850 °C for 2.5 h. After calcination, the mixture was ball milled again and then pressed into disks at a cold-isostatic pressure of 300 MPa. The Cu-doped green pellets were sintered at 1070 °C for 4 h, while the pure KNN pellets were sintered at 1090 °C for 4 h in a K/Na rich ambient. Crystalline structure of the KNN ceramics was examined by x-ray diffraction (Rigaku Co., Japan) with CuK_α radiation on the powder samples. Raman spectrum measurements were performed on a Raman spectrometer under backscattering geometry (HR800, France). An Argon ion laser was used as the excitation source with an output powder of 15 mW at 488 nm. X-band electron paramagnetic resonance (EPR) spectrum was recorded at 3.8 K with a Bruker EMX EPR spectrometer with standard experimental condition. Top and bottom electrodes were made by coating silver paint on both sides of the sintered and polished disks and followed by firing at 550 °C for 20 min. *P-E* loops were measured using a standard ferroelectric analyzer (TF-2000, Aachen, Germany). Poling was conducted at a dc field of 3 kV/mm at

---

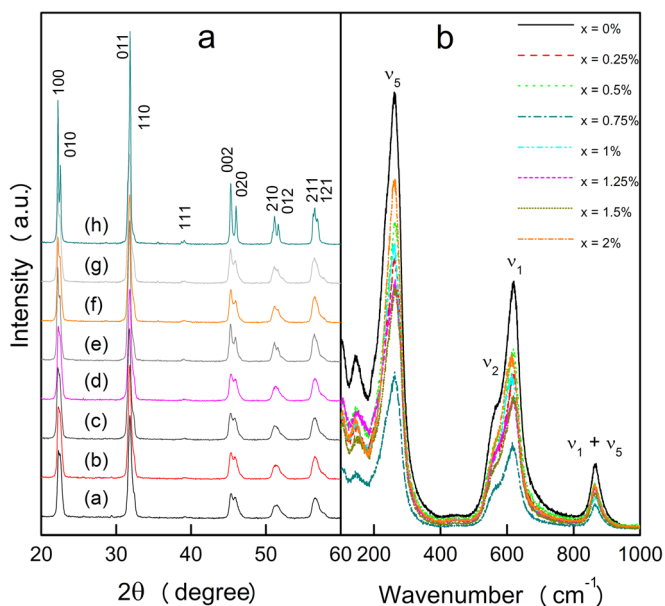a)Author to whom correspondence should be addressed. Electronic mail: aphhuang@polyu.edu.hk.

FIG. 1. XRD and Raman patterns of the KNNC ceramics with x = 0%-2% (a)-(h).

130 °C in a silicone oil bath for 20 min. Dielectric aging behavior was examined by using a frequency-response analyzer (Novocontrol Alpha analyzer) at room temperature. All the samples were held at 550 °C (above $T_C \sim 420$ °C) for 2 h and then cooled immediately to room temperature before the dielectric aging measurement.

Fig. 1 shows XRD and Raman patterns of the KNNC samples. It can be seen that all the KNNC ceramics present a pure perovskite phase at room temperature without a secondary phase, which can be detected within experimental uncertainty. The main Raman vibrations ($\nu_1 \sim \nu_5$) are associated with the BO_6 octahedra and the shift of the stretching mode (ν_1, ν_2) to lower frequencies with increasing amount of Cu could be attributed to a weakening of bond strength caused by the oxygen vacancies.

Fig. 2(a) shows *P-E* loops of selected samples measured at room temperature. Similar to earlier reports,[13] a well-saturated and square-like *P-E* loop is observed for the pure

KNN, with remnant polarization (P_r) of 16.5 μC/cm². However, the *P-E* loop becomes constricted and shows a more pronounced antiferroelectric-like characteristic with increasing Cu content up to x = 0.01. The KNN10 ceramic exhibits a double *P-E* loop with $P_r \sim 0.5 \mu$C/cm². After dc poling only a strongly asymmetric single *P-E* loop was found for the KNN10 [Fig. 2(b)], with a P_r of 16.3 μC/cm². Similar *P-E* loops have been reported for ferroelectrics that contain oriented polarized defects.[11,12] Fig. 2(b) also reveals that a strong internal bias field ($E_{ib} = 0.9$ kV/mm) is established in the KNN10 ceramic during poling. It has been proposed that the defect complex (DC) $(Cu'''_{Nb} - V^{\bullet\bullet}_O)'$ is responsible for the double *P-E* loop in KNN10 (Ref. 13) and is subsequently confirmed by the EPR spectrum.[14,15] Non-switchable DCs that are aligned opposite to the spontaneous polarization (P_s) direction provide the driving force for domain back-switching after the removal of the external electric field, similar to the antiferroelectric behavior. For KNN10, the DCs would be quite mobile at temperatures above 130 °C, and hence the external dc field resulted in a redistribution of the defects and the consequential development of E_{ib}.

It would be expected that higher contents of Cu dopants should create more charged defects and more pronounced double *P-E* loops. Surprisingly, however, only a single *P-E* loop can be observed in the KNN15 and KNN20 ceramics, with greatly enhanced remnant polarizations of 32.2 and 30 μC/cm², respectively, which are twice that of the pure KNN. To understand this abnormal ferroelectric feature, the X-band EPR spectra of KNN15 and KNN10 are compared, as shown in Fig. 3. The EPR results reveal the existence of two distinct Cu^{2+} centers with spin-Hamiltonian parameters $g^1_{zz} = 2.136$ and $g^2_{zz} = 2.232$. According to Eichel *et al.*,[14–16] these correspond to the formation of a dimeric $(Cu'''_{Nb} - V^{\bullet\bullet}_O)'$ (DC1) and a trimeric $(V^{\bullet\bullet}_O - Cu'''_{Nb} - V^{\bullet\bullet}_O)^{\bullet}$ (DC2) defect complex, as schematically shown in Fig. 3. The relative weak resonance signals around $g_{zz} = 2.136$ in KNN15 clearly indicate a lower concentration of DC1.

By employing numerical spectrum simulation,[17] the relative amount of DC1 could be roughly determined to be 80% and 15% for KNN10 and KNN15, respectively. This means
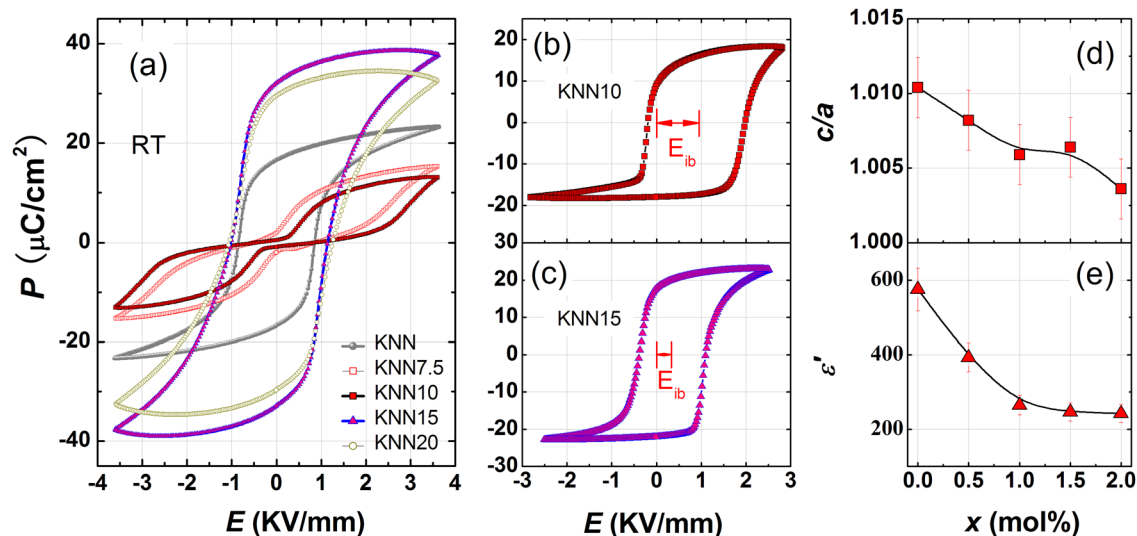

FIG. 2. (a) *P-E* loops of the fresh Cu-doped KNN ceramics measured at 1 Hz and room temperature; (b), (c) *P-E* loops of KNN10 and KNN15 after dc poling; (d), (e) composition dependence of *c/a* ratio and dielectric constant ε' (measured at 100 kHz).
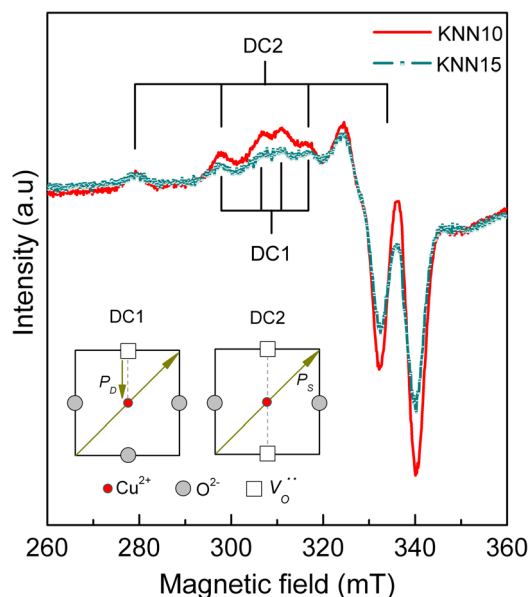
FIG. 3. X-band EPR spectra of KNN10 and KNN15. The inset shows two types of defect structures.

that DC1 dominates in KNN10, while DC2 dominates in KNN15. It is clearly seen that DC1 contains an electric dipole moment (P_D), while the dipole moment for trimeric DC2 almost vanishes due to its symmetric configuration.[14] Because of its non-dipolar nature, DC2 cannot provide enough driving force for domain back-switching and thus did not induce the double *P-E* loops in KNN15.

A slightly constricted *P-E* loop might be expected for KNN15 at room temperature considering the existence of a small portion of DC1. However, the *P-E* loop was not constricted at all. Instead, the polarization was greatly enhanced. In principle, reduced tetragonality [Fig. 2(d)] and less ferro-electric active ions (Nb replaced by Cu) would lead to lower polarization and decreased dielectric permittivity [Fig. 2(e)].

Thus, the enhancement in polarization is not an intrinsic effect. Generally, polarization of ferroelectric ceramics could be contributed extrinsically by their microstructure (such as density and grain size) and space charges. Since the remnant polarization of the KNN15 was suppressed to $20.4\ \mu C/cm^2$ after poling [Fig. 2(c)], which is similar to the value of the saturation polarization of pure KNN, and an internal bias field ($E_{ib} = 0.36$ kV/mm) was also established, it is reasonable to propose that space charge effect is likely responsible for the large enhancement in polarization.

To provide further evidence for the space charge effect, dielectric aging behavior at room temperature was studied. Fig. 4 shows normalized dielectric constant as a function of time for selected KNN ceramics. No obvious aging was observed in pure KNN, while the real part complex dielectric constant ε' of KNN10 decreased by almost 7% in 28 h after annealing. For normal ferroelectrics, the time-dependence of dielectric constant may follow a linear logarithmic law, which is due to the relaxation of domain structure towards an equilibrium configuration.[18] However, it has been found that dielectric aging of KNN10 does not follow a logarithmic law but a stretched exponential equation,[19] which is

$$\varepsilon' = \varepsilon_\infty + \varepsilon_1 \exp[-(t/\tau)^n], \qquad (1)$$

where ε_1 represents the relaxation intensity, the time constant τ reflects the aging rate, and n denotes the distribution of τ. It is well-known that the exponential type of aging behavior generally takes place in relaxor ferroelectrics or a material exhibiting glass or random field behavior. For KNN10, dielectric aging is probably connected to defect-related random field behavior. Contrary to that of KNN10, the dielectric aging of KNN15 and KNN20 displays strong frequency dependence. Meanwhile, the exponential law (Eq. (1)) could not reproduce the data well. A much better fit of the aging behavior can be obtained by the following relationship:
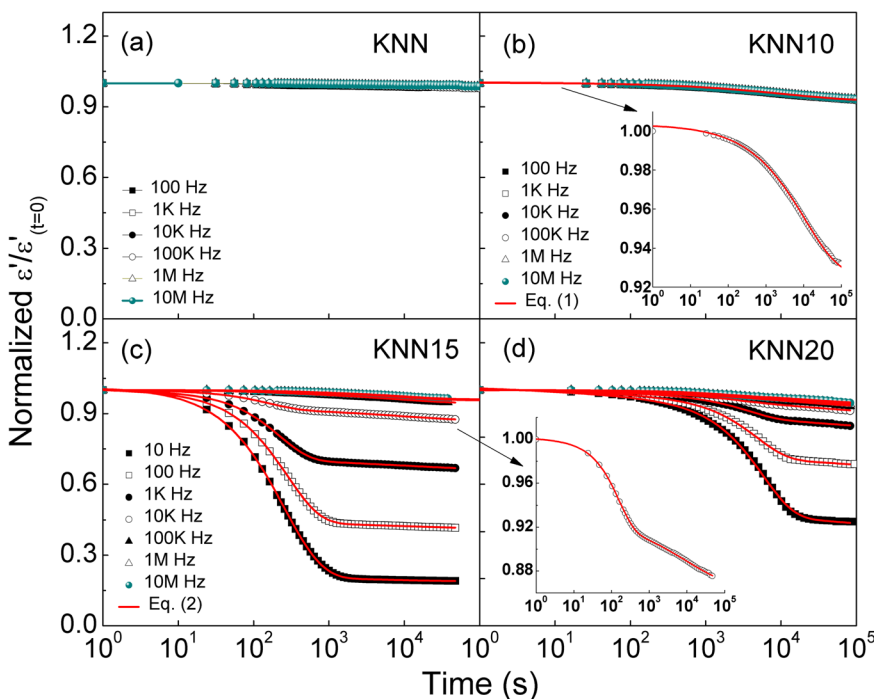

FIG. 4. Time-dependence of normalized dielectric constant of the Cu-doped KNN ceramics. The solid lines are fitting curves according to Eqs. (1) and (2).
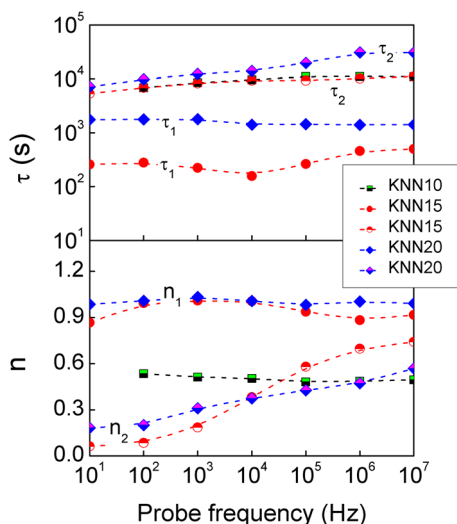
FIG. 5. Parameters obtained by fitting the aging behaviors of the KNN ceramics at different frequency.

$$\varepsilon' = \varepsilon_\infty + \varepsilon_1 \exp[-(t/\tau_1)^{n_1}] + \varepsilon_2 \exp[-(t/\tau_2)^{n_2}]. \quad (2)$$

From Figs. 4(c), 4(d), and 5, it can be seen that the dielectric aging behavior can be well fitted by two exponential functions with two different aging rates: one is fast (τ_1: $10^2 \sim 10^3$ s) and the other is slow (τ_2: 10^4 s). The distribution factor n_1 for the fast process is close to 1, which reveals a Debye-type space charge aging behavior for ferroelectric ceramics. This is also supported by the fact that the fast aging process is only pronounced in the low frequency region, while the slow process dominates the high frequency dielectric response and is accompanied by an increasing n_2 with frequency (Fig. 5).

As aforementioned, the charged DC2s possessed non-polar nature and released electrons, which could gradually move to the domain and/or grain boundaries to form space charges. By contrast, DC1s were accompanied by holes. From first-principles calculations,[20,21] it is known that electrons have much smaller effective mass but much larger mobility than holes in ferro-electric oxides. This explains not only the pronounced space charge effect in the samples with a large amount of DC2 but also their fast aging process. In addition, the polarization of DC1 in KNN15 and KNN20 could be screened by the high mobility space charges, and hence no constricted *P-E* loop was observed. At the boundaries, the space charges provided interface polarization and

then stretched the *P-E* loop. During poling, the applied dc field results in a redistribution of the space charges and the development of an E_{ib} (0.36 kV/mm in KNN15) along the direction of the external field. This is the reason for the shift of the hysteresis curve as shown in Fig. 2(c). It should also be noted that the aligned DC1s should also contribute to the E_{ib} in KNN15 and KNN20.

In summary, we have observed double *P-E* loops in 1 mol. % Cu-doped KNN and single *P-E* loop in 1.5 mol. % and 2 mol. % Cu-doped KNN ceramics. Based on EPR measurements, it is found that the non-switchable $(Cu'''_{Nb} - V^{\bullet\bullet}_O)'$ (DC1) and non-polar $(V^{\bullet\bullet}_O - Cu'''_{Nb} - V^{\bullet\bullet}_O)^\bullet$ (DC2) defect complexes were formed during the ceramic fabrication process. DC1 provided the driving force for domain back-switching to cause the double *P-E* loops in the 1 mol. % Cu-doped KNN, while DC2 contributed to the space charges, which resulted in the enhanced polarization and fast dielectric aging behavior in the 1.5 mol. % and 2 mol. % Cu-doped KNN ceramics.

[1]H. He and X. Tan, Phys. Rev. B **72**, 024102 (2005).
[2]X. Ren, Nat. Mater. **3**, 91 (2004).
[3]P. V. Lambeck and G. H. Jonker, Ferroelectrics **22**, 729 (1978).
[4]W. L. Warren, D. Dimos, B. A. Tuttle, R. D. Nasby, and G. E. Pike, Appl. Phys. Lett. **65**, 1018 (1994).
[5]L. He and D. Vanderbilt, Phys. Rev. B **68**, 134103 (2003).
[6]Yu. A. Genenko, J. Glaun, O. Hirsch, H. Kungl, M. J. Hoffmann, and T. Granzow, Phys. Rev. B **80**, 224109 (2009).
[7]M. Takahashi, Jpn. J. Appl. Phys. **9**, 1236 (1970).
[8]M. I. Morozov and D. Damjanovic, J. Appl. Phys. **107**, 034106 (2010).
[9]M. I. Morozov and D. Damjanovic, J. Appl. Phys. **104**, 034107 (2008).
[10]Y. Y. Guo, M. H. Qin, T. Wei, K. F. Wang, and J. M. Liu, Appl. Phys. Lett. **97**, 112906 (2010).
[11]Q. Tan and D. Viehland, J. Am. Ceram. Soc. **81**, 328 (1998).
[12]Q. Tan, J. Li, and D. Viehland, Appl. Phys. Lett. **75**, 418 (1999).
[13]D. M. Lin, K. W. Kwok, and H. L. W. Chan, Appl. Phys. Lett. **90**, 232903 (2007).
[14]R.-A. Eichel, E. Erünal, M. D. Drahus, D. M. Smyth, J. V. Tol, J. Acker, H. Kungl, and M. J. Hoffmann, Phys. Chem. Chem. Phys. **11**, 8698 (2009).
[15]R.-A. Eichel, Phys. Chem. Chem. Phys. **13**, 368 (2011).
[16]E. Erünal, R.-A. Eichel, S. Körbel, C. Elsässer, J. Acker, H. Kungl, and M. J. Hoffmann, Funct. Mater. Lett. **3**, 19 (2010).
[17]S. Stoll and A. Schweiger, J. Magn. Reson. **178**, 42 (2006).
[18]W. A. Schulze and K. Ogino, Ferroelectrics **87**, 361 (1988).
[19]Q. M. Zhang, J. Zhao, and L. E. Cross, J. Appl. Phys. **79**, 3181 (1996).
[20]T. Qi, I. Grinberg, and A. Rappe, Phys. Rev. B **83**, 224108 (2011).
[21]D. Bagayoko, G. L. Zhao, J. D. Fan, and J. T. Wang, J. Phys.: Condens. Matter **10**, 5645 (1998).